Channel-Adaptive Location-Assisted Wake-up Signal Detection Approach Based on LFM Over Underwater Acoustic Channels

DEQING WANG, **HAIYU LI**, **YONGJUN XIE**, **XIAOYI HU**, **AND LIQUN FU**, **(Senior Member, IEEE)**
Key Laboratory of Underwater Acoustic Communication and Marine Information Technology, Xiamen University, Ministry of Education, Xiamen 361005, China
School of Information Science and Engineering, Xiamen University, Xiamen 361005, China

Corresponding author: Liqun Fu (liqun@xmu.edu.cn)

ABSTRACT This paper focuses on the wake-up signal detection design for underwater acoustic communication (UAC) terminals. A wake-up signal detection unit can considerably reduce the power consumption of the terminals. Compared with terrestrial wireless counterparts, the wake-up signal detection design for UAC terminals is challenged by the severe underwater acoustic channels, which is characterized as doubly selective fading and low signal-to-noise ratio (SNR). This paper proposes a wake-up signal detection approach called channel-adaptive detection and location-assisted joint decision (ChAD-LaJD), for UAC terminals. ChAD-LaJD applies a group of linear frequency modulation (LFM) signals as a wake-up signal. In order to increase the detection probability while keeping a low false alarm rate, ChAD-LaJD consists of two procedures: channel-adaptive detection (ChAD) and location-assisted joint decision (LaJD). Besides a pre-determined threshold, ChAD procedure defines two special parameters which reflect instantaneous channel states to detect wake-up signals adaptively. LaJD procedure further exploits the location relationships of LFM signals detected by ChAD to achieve a joint decision. The simulations and field experiments are conducted to evaluate the performance of ChAD-LaJD. The results show that ChAD-LaJD outperforms the conventional methods that consider a fixed threshold (FixTh) and/or constant false alarm rate (CFAR).

INDEX TERMS Underwater acoustic channels, wake-up, linear frequency modulation, channel-adaptive.

I. INTRODUCTION

Underwater acoustic communication (UAC) or underwater acoustic sensor networks (UASNs) have attracted much research interest in recent years because of their wide range of potential applications, such as marine resources exploitation, industrial instrumentation and control, military surveillance, and security monitoring [1], [2]. Compared with the terrestrial wireless communication systems, energy efficiency becomes even more critical for UAC or UASNs where underwater acoustic terminals rely on non-rechargeable and unchangeable batteries to provide essential power for long-term sensing, data collection, and communications [3]. Therefore, it is important to develop effective power saving mechanisms for UAC terminals so that energy conservation can be achieved and the lifetime of UASNs can be extended.

Among existing power saving mechanisms, wake-up mechanisms for UAC terminals play an important role in reducing the power consumption and extending the battery life. UAC terminals with wake-up ability consume less energy in the idle listening mode. However, the design of underwater acoustic wake-up mechanism is challenged by the severe underwater acoustic channels, which are characterized as doubly-selective fading and high ambient noise. The wake-up mechanisms are required to combat the doubly-selective fading and low signal-to-noise ratio (SNR) [4]. Furthermore, compared with frame synchronization, the wake-up mechanisms are usually based on low power devices, resulting in weak processing ability.

The associate editor coordinating the review of this manuscript and approving it for publication was Emrecan Demirors.

Most literatures for underwater acoustic detection systems focus on detection probability and energy efficiency. Some detection methods based on low-power chip with weak processing ability are presented. In [5], ID detection IC AS3933 is used to handle acoustic hydrophone inputs. The chip AS3933 is a commercial integrated circuit which is designed for active RFID tags with low power consumption. It wakes up the system if a particular carrier is sensed. However, the chip AS3933 is not suitable for combating multi-path inter-symbol interference (ISI) channel since it is lack of any built in mechanisms to deal with ISI. Applying the same wake-up signal, i.e., a single-frequency, a design of low-power wake-up circuits based on SCM C8051F020 has been proposed in [6]. The circuits collect the wake-up signal and identify the frequency by making single point of fixed-point Discrete Fourier Transform (DFT). But the performance of this wake-up scheme is only evaluated under the Gaussian white noise channels. The authors in [7] proposed a low-complexity wake-up receiver using a TI MCU called MSP430F5529 for UASNs. By using dual pseudo-random noise (PN) sequences, the wake-up mechanism is designed based on autocorrelation to reduce the complexity. The proposed dual PN detection scheme has been tested in long multi-path channels with more than 60 taps. However, the time-selective characteristics of underwater acoustic channel destroy the autocorrelation properties of PN sequences, resulting in low detection probability.

Different from single-frequency or PN sequences mentioned above, linear frequency modulation (LFM) signals have been used for frame synchronization [8], random access [9], communication [10], and parameter estimation [11] because of its good autocorrelation and Doppler tolerance in doubly-selective fading channels. The cut along the delay axis of the autocorrelation is very steep, which is conductive to signal detection. Traditional detection methods for LFM signals are based on a replica correlation (RC) detector [12], [13]. The LFM signal is assumed to be detected when the correlation output between the received signal and the replica of the transmitted signal is greater than a pre-determined threshold. In order to separate the overlapping LFM signals, a method based on Fractional Fourier Transform (FrFT) is applied in all kinds of signal processing applications. FrFT is a generalization of the classical Fourier transform and can be interpreted as a rotation in the time-frequency plane. In the FrFT domain, an LFM signal can be represented as an impulse at an appropriate time-frequency rotation angle since the transform kernel is a set of chirp bases [14]. However, the FrFT-based detection methods are much more complicated than the traditional correlation-based ones, resulting in computational burden for the receivers with weak processing ability. Furthermore, the detection probability and the false alarm rate are more important rather than accurate parameters estimation in wake-up signal detection systems.

Most aforementioned methods are based on RC technique. The biggest challenge is that the prefixed threshold cannot adapt to the time-varying background, leading to a high false alarm rate. In order to compute detection thresholds and minimize the impact of the background on the false alarm rate, common false alarm rate (CFAR) technique has been developed [15]. Usually, existing CFAR detection procedures are performed using sliding windows, from which the parameters of the hypothesized model are estimated, and the data available in the reference window are employed to compute the decision threshold. Ref. [16], [17] applied CFAR technique in underwater acoustic signal detection. Inspired by it, we adopt this idea and further improve it to develop our wake-up signal detection approach.

In this paper, we propose a novel LFM-based wake-up signal detection approach named as Channel-Adaptive Detection Location-assisted Joint Decision (ChAD-LaJD) for UAC terminals. ChAD-LaJD aims to increase the detection probability while keeping a low false alarm rate over doubly-selective underwater acoustic channels. Its main characteristics are listed as follows.

- A group of LFM signals are applied as a wake-up signal. Furthermore, these LFM signals are detected applying simple RC technique to reduce the computational complexity.
- Besides a prefixed threshold V_{th}, two special parameters, denoted by α and β, are defined to reflect instantaneous channel states. The channel states include multi-path structure, ambient noise, sidelobes resulted by correlation and so on.
- It is a two-stage approach implemented by two procedures called ChAD and LaJD, respectively. ChAD detects the correlation peaks applying the parameter set $\{V_{th}^*, \alpha^*, \beta^*\}$. LaJD further makes a decision whether a wake-up signal is arrived or not according to the location relationship of the correlation peaks. Two algorithms are presented for ChAD and LaJD procedures, respectively.

Compared with the RC-based detection method [7], ChAD-LaJD does not require a precise threshold. Furthermore, it is suitable for the doubly-selective channels, while the traditional detection methods applying common false alarm rate technique [16] only consider ambient noise. In order to evaluation the performance of ChAD-LaJD, simulation and field trials are conducted. First, the simulations applying doubly-selective channels are carried out to achieve the optimal parameter set $\{V_{th}^*, \alpha^*, \beta^*\}$. The results show that the detection probability and the false alarm rate are both better than the convention methods as long as V_{th}^* is set to a comparative low value. We further conduct the sea and lake trials to evaluate the performance of ChAD-LaJD. The channels in the sea trials are with simple multi-path structure but with Doppler effect; while the channels in the lake trials are with complicated multi-path structure. It can be shown that ChAD-LaJD outperforms the conventional methods under both channels with significant differences.

The rest of this paper is organized as follows. Section II describes the system model. In Section III, we introduce the wake-up signal detection approach. Simulations and
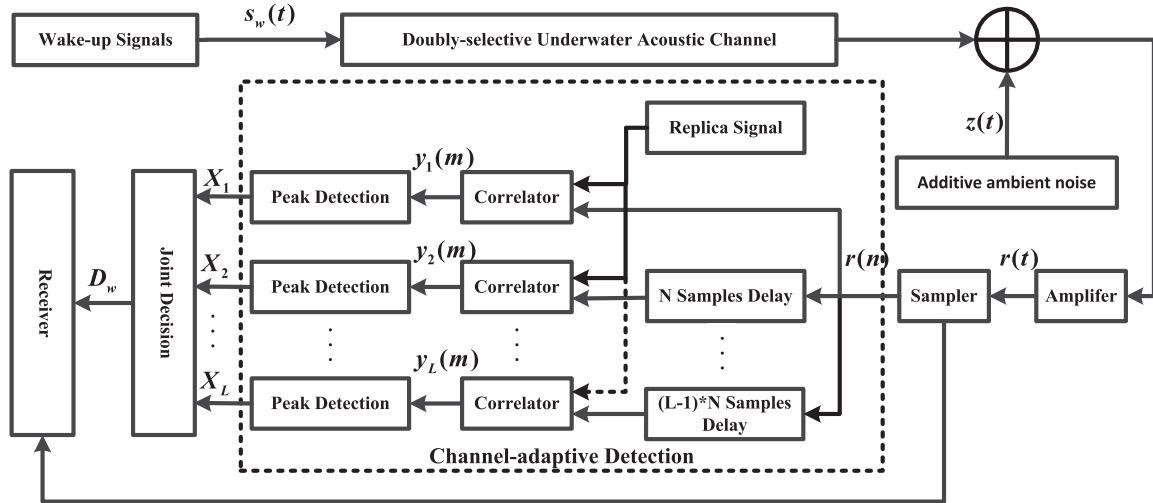
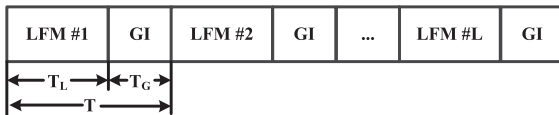**FIGURE 1.** The wake-up signal detection system.

FIGURE 2. The structure of a wake-up signal.

experimental results are presented in Section IV and Section V, respectively. Finally, conclusions are given in Section VI.

II. SYSTEM MODEL

We consider a wake-up signal detection system which is independent of the receiver over underwater acoustic channels. The system aims to decide whether wake-up signals are arrived or not with low energy consumption. If a wake-up signal is detected, the receiver will wake up from the sleeping mode. Compared with the traditional circuits-based design, the system design is based on a digital signal processing (DSP) chip such as TMS320C6748 whose power consumption is $426.93mW$ with the processing capability of 2746 MFLOPS [18], [19]. This chip has been applied in low power DSP platform design [20]. Aided by the low-power DSP chip, more complex detection methods can be applied with low energy consumption. In the following, we will introduce the design framework and the underwater acoustic channel model, respectively.

A. OVERVIEW OF THE DESIGN

The wake-up signal detection system is depicted in Fig. 1. At the transmitter side, L adjacent LFMs are used as a wake-up signal, as shown in Fig. 2. These LFMs are separated by a Guard Interval (GI). The length of each LFM pulse and GI are set as T_L and T_G, respectively. An LFM symbol consists of an LFM pulse and a GI, with a length of $T = T_L + T_G$. After passing through a doubly-selective underwater acoustic

channel with additive ambient noise, the received wake-up signal is amplified and sampled to be a discrete-time serial which will be buffered into a low-power DSP chip. Then a detection approach is conducted to decide whether wake-up signals are arrived or not based on the buffered data serial. It consists of two parts including Channel-Adaptive Detection (ChAD) and Location-assisted Joint Decision (LaJD). ChAD procedure is performed in parallel branches whose number is the same as the number of LFMs. The l-th branch detects the l-th LFM by applying a correlator to the corresponding delayed discrete-time serial. As a result, the corresponding locations of the transmitted LFMs can be obtained after ChAD procedure. Following up ChAD, LaJD decides whether wake-up signals are arrived or not by exploring the location relationships of the detected LFMs. Compared with the detection method using a single LFM based on Microcontroller Unit (MCU), our design builds up a wake-up signal using multiple LFMs. Furthermore, the location relationship of these LFMs are exploited. The ChAD and LaJD can be easily implemented with a low-power DSP chip, which requires only a little more computation and memory than those MCU-based detection systems [6], [7].

B. CHANNEL MODEL AND INPUT-OUTPUT RELATIONSHIP

Suppose that the l-th passband LFM signal in a wake-up signal is given by

$$s_l(t) = \exp\{j2\pi f_0 t + j\pi \mu t^2\}, \quad 0 \le t \le T_L, \quad (1)$$

where f_0 is the initial frequency and μ is the frequency rate, which is equal to $\frac{B}{T_L}$, in which B is the bandwidth. The instantaneous frequency is $f(t) = f_0 + \mu t$. Thus, a wake-up signal can be expressed as

$$s_w(t) = \sum_{l=0}^{L-1} s_l(t - lT), \quad (2)$$

where L is the number of LFMs.

Consider a typical doubly-selective underwater acoustic channel whose channel impulse response (CIR) is

$$h(t; \tau) = \sum_{\ell=1}^{N_\ell} A_\ell(t)\delta(\tau - \tau_\ell - at), \quad (3)$$

where N_ℓ is the number of channel paths, $A_\ell(t)$ and τ_ℓ are the amplitude gain and the delay associated with the ℓ-th path, respectively. The Doppler scaling factor is denoted by a, which is the same for all paths. In order to optimize the decision parameters, two different channel models, called Amplitude Constant (AC) Channel [21] and Amplitude Stochastic (AS) Channel [4], are applied in this paper. The path amplitudes are assumed to be constant during the period of a wake-up signal in AC Channel, i.e., $A_\ell(t) \simeq A_\ell$. While $A_\ell(t)$ in AS Channel is changing over time. As for other parameters in Equ. (3), we assume that the path delays are constant during the period of a wake-up signal. After passing through the channel, the wake-up signal at the receiver can be expressed by the linear time varying convolution of $s_w(t)$ and $h(t; \tau)$ in the presence of additive ambient noise $z(t)$:

$$r(t) = s_w(t) * h(t; \tau) + z(t). \quad (4)$$

After sampling with interval T_S, the received wake-up signal $r(t)$ can be expressed by a discrete-time serial:

$$r(n) = \sum_{k=0}^{K-1} h(n; k)s_w(n-k) + z(n), \quad (5)$$

where K is the length of CIR, and n and k denote the index for time and delay, respectively. We use RC detector, called Correlator shown in Fig. 1, to search for the LFMs according to the correlation peaks [13]. As there are multiple LFMs in a wake-up signal, multiple correlation peaks may be obtained. As shown in Fig. 1, the correlator in a branch is only correlated with its corresponding replica of the transmitted LFM. The output of the l-th correlator is

$$y_l(m) = \left| \sqrt{\frac{2}{N}} \sum_{i=0}^{N_L-1} s_l^*(i)r(i + m + (l-1)N) \right|^2, \quad (6)$$

where N and N_L are the sample length between two adjacent LFMs and the length of the discrete-time LFM signal, respectively. We have $N = \frac{T}{T_S}$ and $N_L = \frac{T_L}{T_S}$. And then these correlation outputs are sent to Peak Detection to get the locations of the LFMs. Ideally, L peaks will be detected by the following operation,

$$X_l = \arg\max_m y_l(m) + (l-1)N, \quad (7)$$

where X_l is the location of the l-th LFM signal. Since the searching range for m may vary with the searching starting point, it will be detailed introduced in Subsection III-A. After getting X_l, the LaJD process is applied to decide whether a wake-up signal is arrived or not:

$$D_w = f(X_1, \dots, X_L), \quad (8)$$

where $f(\cdot)$ is a self-defined detect operation that will be realized by Algorithm 2 in Subsection III-B. The output D_w is a binary value. If the received signal is detected as a wake-up signal, the output $D_w = 1$; otherwise $D_w = 0$.

In the subsequent sections, we evaluate the performance of the detection probability P_D and the false alarm rate P_{FA}, respectively.

III. DETECTION APPROACHES
A. CHANNEL ADAPTIVE DETECTION

In order to detect LFMs and their corresponding locations, ChAD procedure tries to get a real peak from the RC outputs. Given a comparatively ideal channel, with high SNR, short multi-path spread and weak Doppler effect, the correlation peak is clear because of LFM's good autocorrelation characteristics. However, underwater acoustic channels are featured by three factors, i.e., long multi-path spread, severe Doppler effect, and low SNR. The peak is not clear over underwater acoustic channels. Fig. 3 shows a typical correlation output from sea trials. We can observe multiple peaks with different values. We treat the maximal one as the real peak which should be detected and the other peaks as the false ones. In the conventional detection method with fixed threshold V_{th}, if V_{th} is set to be a low value, the false peaks are greater than V_{th}, which results in false alarms and high P_{FA}. Conversely, if V_{th} is set to be a high value, the real peak cannot be detected, which leads to a low P_D. In order to better detect the real peak, besides V_{th}, we further define two special parameters α and β that reflect the instantaneous channel states:

$$\begin{cases} \alpha = \dfrac{V_{pp}}{V_{Nmean}}, \\ \beta = \dfrac{V_{pp}}{max\{V_{Lpp}, V_{Rpp}\}}, \end{cases} \quad (9)$$

where V_{pp}, V_{Lpp}, V_{Rpp} and V_{Nmean} are the maximum peak, the left sidelobe peak, the right sidelobe peak, and the mean power of the ambinet noise, respectively. The parameters α and β are called noise normalized peak and sidelobe normalized peak, respectively. The parameter β reflects the relationship between V_{pp} and the sidelobe peaks. According to the results of simulations and experiments, the sidelobe peaks are affected by three factors ,i.e., multi-path spread, pulse noise, and correlation sidelobe. When a wake-up signal is arrived, V_{pp} should be much greater than the sidelobe peaks V_{Lpp} or V_{Rpp}, i.e., β is greater than one. Thus, the preparative task of the detection approach is to find an optimal set $\{V_{th}^*, \alpha^*, \beta^*\}$. However, maximizing P_D and minimizing P_{FA} are paradoxical at the same set $\{V_{th}, \alpha, \beta\}$. In this paper, the optimal parameter set $\{V_{th}^*, \alpha^*, \beta^*\}$ is obtained with simulations under two different channel models, as shown in Section IV.

With the optimal parameter set $\{V_{th}^*, \alpha^*, \beta^*\}$, ChAD applies multiple parallel branches to get the locations of the LFMs, i.e., $X_1, X_2, \dots, X_L$, as shown in Fig. 1. The l-th branch for detecting the l-th LFM is illustrated in Fig. 4.
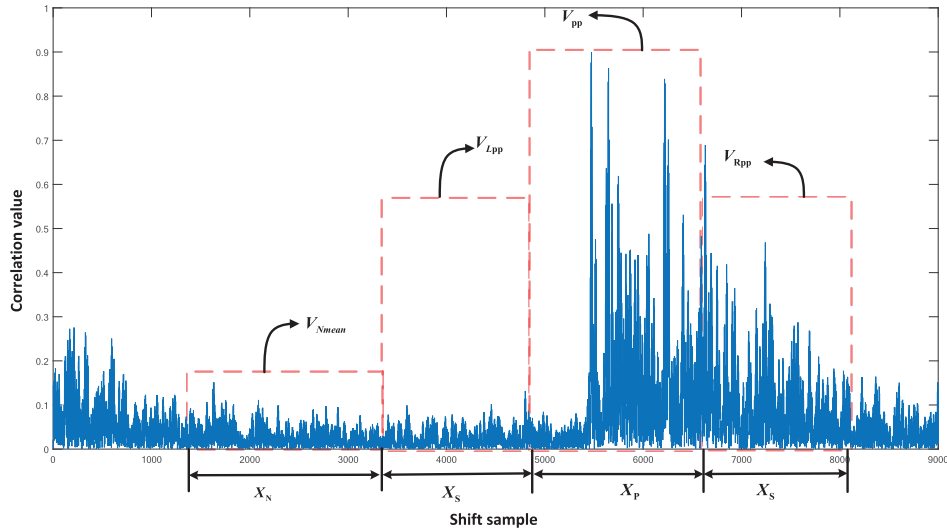
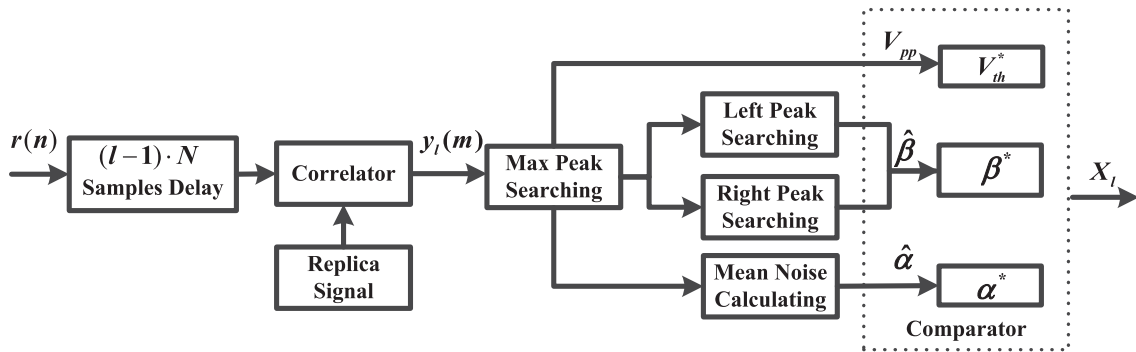**FIGURE 3.** LFM peak detection windows.

FIGURE 4. The block diagram of channel-adaptive detection.

When detecting the *l*-th LFM, the discrete serial $\{r(n)\}$ should be offset by $(l-1)N$ samples. Then, a local replica signal $s_l^*(n)$ is used to correlate with the offset discrete serial $r(n + (l - 1)N)$ to get the *l*-th correlation values $\{y_l(m)\}$. The aforementioned operation is shown by Equ. (6) in Subsection II-B. Following up correlation, V_{pp} is detected from $\{y_l(m)\}$, and then its location X_l is used as the reference point of searching window to obtain other values including V_{Lpp}, V_{Rpp} and V_{Nmean}. Then the measured parameters $\hat{\alpha} = \frac{V_{pp}}{V_{Nmean}}$ and $\hat{\beta} = \frac{V_{pp}}{max\{V_{Lpp}, V_{Rpp}\}}$ are sent to a comparator together with V_{pp}. The comparator outputs the location X_l of the *l*-th LFM if the following conditions are satisfied:

$$\begin{cases} V_{pp} > V_{th}^*, \\ \hat{\alpha} > \alpha^*, \\ \hat{\beta} > \beta^*. \end{cases} \quad (10)$$

How to obtain V_{pp}, V_{Lpp}, V_{Rpp} and V_{Nmean} is a key issue for peak detection. The challenge comes from the arrival uncertainty of V_{pp} and its consequent buffer arrangement. The detailed detection method of the *l*-th branch is as follows.

First, a detection window is set according to the location of V_{pp}, i.e., X_l. Then the correlation outputs $y_l(m)$ slide into the detection window, as shown in Fig. 3. Suppose that the serial in the detection window is *u*. In addition, the covering periods for V_{Nmean}, V_{Lpp} or V_{Rpp} and V_{pp} are X_N, X_S and X_P, respectively. The values of X_N, X_S and X_P are decided by the channel states. Ideally, X_P is the period of window for searching V_{pp}. It should cover the delay spread so as to decrease the impact by multi-paths. But the channel spread is not a fixed value available in advance. So we choose an experience one in real operation. In this paper, we set X_P as 1600 samples, corresponding with $40ms$ at sample rate $40kHz$. The period of window X_S for searching V_{Lpp} or V_{Rpp} does not need to be strictly set. Setting X_S to be 200 samples are enough in our system. The period of window X_N for calculating V_{Nmean} is set as 3200 samples. The length of the detection window M is the sum of X_N, X_S and X_P. The values of V_{pp}, V_{Lpp}, V_{Rpp} and V_{Nmean} are updated at each iteration based on *u*. As a result, $\hat{\alpha}$ and $\hat{\beta}$ can be obtained to be compared with the prefixed parameters. If the detection conditions are not satisfied, the next iteration starts. The detailed steps are

---

Algorithm 1 Peak Detection for the l-th Branch

Input:

    1) The l-th discrete received signal y_l;

    2) Prefixed parameters V_{th}^*, α^* and β^*;

    3) Detection window length M;

    4) Covering periods X_N, X_S and X_P.

Output: The location of V_{pp}: X_l

Initialize

    $X_l = 0$, $\hat{\alpha} = 0$, $\hat{\beta} = 0$;

    $u \leftarrow y_l[0 : M - 1]$.

repeat

$\quad$ $V_{pp} = \max u$;

$\quad$ $X_l = \arg \max_n u(n)$;

$\quad$ $u \leftarrow y_l\left[X_l - \frac{X_p}{2} - X_N - X_S : X_l + \frac{X_p}{2} + X_S\right]$;

$\quad$ $V_{Lpp} = \max u\,[X_N : X_N + X_S]$;

$\quad$ $V_{Rpp} = \max u\left[X_l + \frac{X_p}{2} : M\right]$;

$\quad$ $V_{Nmean} = \overline{u\,[0 : X_N]}$;

$\quad$ $\hat{\alpha} = \frac{V_{pp}}{V_{Nmean}}$;

$\quad$ $\hat{\beta} = \frac{V_{pp}}{max\{V_{Lpp}, V_{Rpp}\}}$;

$\quad$ $u \leftarrow y_l\left[X_l - \frac{3X_p}{2} - X_N + X_S : X_l + \frac{3X_p}{2} + 2X_S\right]$.

until $V_{pp} > V_{th}^*$ *and* $\hat{\alpha} > \alpha^*$ *and* $\hat{\beta} > \beta^*$;

return X_l.

---

summarized in Algorithm 1. What should be noted is that $X_P + 2X_S$ samples instead of one are shifted into the detection window in the next iteration if no peak is detected. It increases the detection speed.

B. LOCATION-ASSISTED JOINT DECISION

Besides ChAD, LaJD procedure is another part of ChAD-LaJD. Due to doubly-selective characteristics of underwater acoustic channels, some LFMs may not be detected. On the other hand, some multi-paths or pulse noise are falsely detected. The former decreases P_D and the latter increases P_{FA}. In this paper, L adjacent LFMs instead of one are used as a wake-up signal to increase P_D while keeping P_{FA} low. First, LaJD procedure gets multiple locations corresponding to the transmitted LFMs from ChAD. Then it takes the relationship of the locations into account. Based on the relationship, LaJD outputs $D_w = 1$ to wake-up the receiver. The key issue in LaJD is how to construct the location relationship.

Without loss of generality, suppose that a wake-up signal consists of three LFMs. First, we consider an ideal situation called Case 1 to illustrate how LaJD constructs a function to get D_w as shown in Equ. (8). As shown in Fig. 5, three LFMs are all correctly detected by ChAD. Their corresponding locations are X_1, X_2 and X_3, respectively. Ignoring the difference of signal paths, the locations of LFMs are only influenced by Doppler effect. In this paper, The Doppler effect are reflected by the Doppler scaling factor a presented
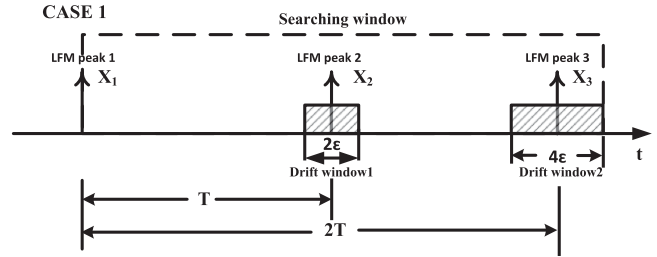

FIGURE 5. Joint decision case I: All LFMs are detected.
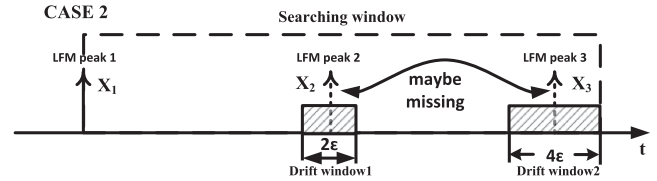

FIGURE 6. Joint decision case II: An LFM is missing.

in Equ. (3). As a result, a signal with length T will be compressed or expanded to $(1 + |a|)T$. If X_1 is considered as a referential position, X_2 will appear at $X_1 + aT$. For the convenience of expression, the absolute value of aT is denoted as ε, i.e., X_2 will drift at the range between $X_1 - \varepsilon$ and $X_1 + \varepsilon$. The range is defined as drift window shown in Fig. 5. Similarly, X_3 will drift at the range between $X_1 - 2\varepsilon$ and $X_1 + 2\varepsilon$. In other words, LaJD takes Doppler effects into account in the decision procedure. Suppose that the receiver can be waken-up if at least two LFMs are detected. Then we can construct the following function to get the value of D_w:

$$D_w = \begin{cases} 1, & \text{if C1 or C2 or C3 holds,} \\ 0, & \text{otherwise,} \end{cases} \quad (11)$$

where

$$\begin{cases} C1 : T - \varepsilon \leq X_2 - X_1 \leq T + \varepsilon; \\ C2 : T - \varepsilon \leq X_3 - X_2 \leq T + \varepsilon; \\ C3 : 2T - 2\varepsilon \leq X_3 - X_1 \leq 2T + 2\varepsilon. \end{cases} \quad (12)$$

The conditions C1, C2 and C3 stand for the location relationships between two LFMs among the wake-up signal. Due to the fading features of underwater acoustic channels, some LFMs may not be detected. This situation is illustrated in Fig. 6 and called Case 2. After detecting the first LFM, the second LFM or the third LFM (denoted by the dotted arrows in Fig. 6) is missing. However, as long as another LFM except the first one is detected, LaJD still outputs $D_w = 1$ because C2 or C3 is satisfied.

A more complicated situation called Case 3 is shown in Fig. 7. In this situation, after detecting the first LFM, another LFM is detected at an undesirable position, i.e., beyond the drift window. This happens when some LFMs are falsely detected. LaJD will drop the first position X_1 and reset X_2 as the starting point in a new searching window. This case will be discussed in details in lake trials in Subsection V-B. Given the locations of correlation peaks $\{X_l\}$, $l = 1, 2, \ldots$,
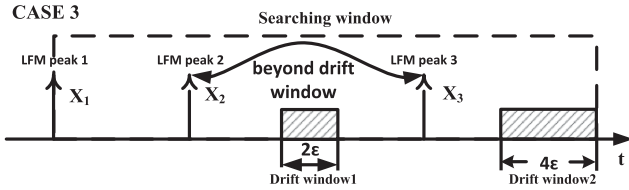
FIGURE 7. Joint decision case III: Undesired signal is detected.

Algorithm 2 Joint Decision

Input: The locations of peaks $\{X_l\}, l = 1, 2, \ldots$
Output: The value of decision result D_w
Initialize
    $D_w \leftarrow 0;$
    $j \leftarrow 0.$
repeat
        $X_1 \leftarrow X_{j+1};$
        $X_2 \leftarrow X_{j+2};$
        $X_3 \leftarrow X_{j+3};$
        $j = j + 1;$
        if *C1 or C2 or C3* **then**
          | Do $D_w \leftarrow 1$
        end
until $D_w == 1;$
return $D_w.$

---

the decision making of the wake-up signal is summarized in Algorithm 2.

C. COMPUTATIONAL COMPLEXITY

The most computational complexity of ChAD-LaJD comes from L correlators in ChAD procedure. The sample rate f_s is $1/T_s$. According to the definitions in Subsection II-B, the length of the sampled LFM is N_L. Therefore, $f_s * N_L * L$ multiply-add operations are required per second. Given the parameters $f_s = 40kHz$, $N_L = 2560$, and $L = 3$, there are 307.2 million multiply-add operations per second. It is far beyond the processing capability of MCU such as MSP430 chip [22] , which is often used in low power applications. On the contrary, with the processing capability of 2746 MFLOPS, TMS320C6748 is capable enough to handle these multiply-add operations. Furthermore, the power consumption is about $43mW$, one tenth of the full power consumption $426.93\ mW$.

IV. SIMULATIONS

First, we illustrate the characteristics of LFM signals. Furthermore, we obtain the optimal decision parameters with simulations under two different channel models. Based on the optimal parameter set, the detection probability and the false alarm rate are evaluated.

A. CHARACTERSITICS OF LFM SIGNALS

The parameters of LFM signals are listed in TABLE 1. Fig. 8a shows the LFM signal with pulse width N_L in time-domain.

TABLE 1. The parameters of LFM signals in simulations.

Parameters	Values
Number of LFMs L	3
Length of each LFM T_L (ms)	64
Guard interval T_G (ms)	32
Initial frequency f_0 (kHz)	2.5
Center frequency f_c (kHz)	4
Bandwidth B (kHz)	3
Sample rate f_s (kHz)	40

(a) Signal in time-domain   (b) Relationship between time and frequency

FIGURE 8. LFM signal.

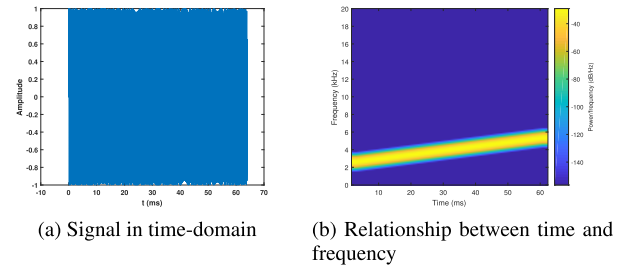(a) Zero Doppler ambiguity of LFM and a single pulse   (b) Timing accuracy caused by Doppler shift
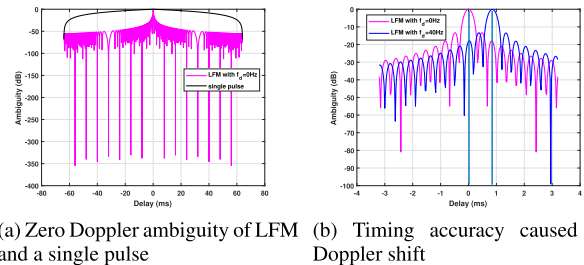
FIGURE 9. Ambiguity function of LFM signals.

Fig. 8b illustrates the relationship between time and frequency. Compared with other prone signals, such as sinusoid with a limited duration, the frequency of the LFM signal is swept linearly across the pulse width. So the LFM signal has a nonzero spectrum, which is prone to resisting deep fading in frequency-domain. Fig. 9a shows the differences of zero Doppler ambiguity between the LFM signal and a signal pulse modulated by a sinusoid whose frequency is f_c. The cut along the delay axis of the LFM signal changes much more significantly than the one of single pulse. That is, the LFM signal is with better autocorrelation characteristics, which is beneficial to get accurate peak position in RC detector.

Based on the aforementioned characteristics, LFM signals are superior as wake-up signals in doubly selective underwater channels. However, in the presence of Doppler spread, the received LFM signal and the transmitted LFM signal mismatch, resulting in the decrease of timing accuracy. Fig. 9b shows the impacts caused by Doppler shift. About $1ms$ timing offset is obtained when Doppler shift is $f_d = 40Hz$ at the center frequency $f_c = 4kHz$, or 40 samples offset at the sample rate $f_s = 40kHz$. This characteristic has been considered in the LaJD procedure. The samples offset caused by Doppler shift is taken into account through the drift windows in the
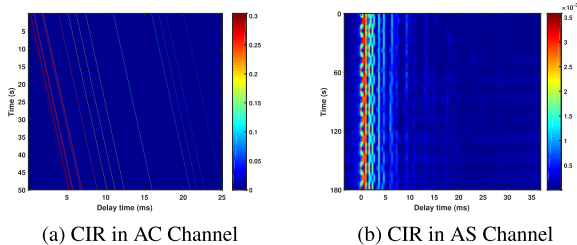
(a) CIR in AC Channel (b) CIR in AS Channel

FIGURE 10. CIRs in simulations.

LaJD procedure. Thus, Doppler shifts are not considered in the subsequent simulations and trials any more.

B. OPTIMIZING PARAMETERS

In this subsection, we obtain the optimal parameter set $\{V_{th}^*, \alpha^*, \beta^*\}$ with simulations under two different channel models, called AC and AS Channel, respectively. The other parameters including X_N, X_S, X_P used in ChAD procedure and ε used in LaJD procedure are set in Subsection III-A and Subsection III-B, respectively. The two channel models are generated according to Equ. (3). AC Channel consists of $N_\ell = 20$ paths whose amplitudes and delays are in accordance with first-order statistical properties of underwater acoustic channel. The inter-arrival time of consecutive paths, $\tau_\ell - \tau_{\ell-1}$, is exponentially distributed with the mean of $1ms$, resulting in a $20ms$ channel delay spread on average. The amplitudes A_ℓ are independent and Gaussian distributed with the average power decreasing exponentially with the delay, where the power difference from 0 to 20 ms is $15dB$ [21]. Besides the aforementioned parameters, the Doppler scaling factor is set as $a = 1 \times 10^{-3}$. A certain CIR of AC Channel is shown in Fig. 10a.

AS Channel is based on beam tracing tools such as Bellhop to get the path number given the environment conditions. The amplitudes and the delays are derived from underwater statistical characterization on large- and small-scale effects [4], in which each propagation path is modeled by a large-scale gain and micro-multipath components that

cumulatively result in a complex Gaussian distortion $A_\ell(t)$. The primary parameters of the environment conditions are list as follows. The water depth and the transmission range are $100m$ and $10km$, respectively. The frequency band of signal is same as the one of LFM signals, i.e., from $2.5kHz$ to $5.5kHz$. The variances of small-scale surface and bottom variations are 1.125 and 0.563, respectively. Fig. 10b shows the CIR of AS Channel. Compared with AC Channel, the CIR is obtained after mitigating the dominated Doppler scaling factor, but the amplitude of each path is still changing with time.

The optimal parameter set $\{V_{th}^*, \alpha^*, \beta^*\}$ is determined as follows. First, we vary α and β with and without input signals to decide the optimal values α^* and β^*. Fig. 11 and Fig. 12 show the mean values and the bounds of 10000 simulations in AC and AS Channels, respectively. The bounds are defined as the maximum and minimum values in the simulations at the same SNR. As shown in Fig. 11a and Fig. 12a, the mean values of α when a signal passes through the channels are greater than the ones without input signals. At the same time, α varies between the maximum and minimum values due to the randomness of noise at the same SNR. A greater mean value of α with signal can be obtained at a higher SNR, while the mean values only with noise are stable. It is reasonable since α reflects the ratio between the received signal power and the additive noise power. In general, the optimal values of α should be less than the maximum value at any SNRs for a lower P_{FA}. However, lower α will result in higher P_D. So we set $\alpha^* = 6$ after considering the trade-off between P_D and P_{FA}.

Compared with α, β reflects the ratio between the signal peak and sidelobe peaks. The variation of β is more severe at all SNRs without signal because of the randomness of noise. This phenomenon is shown in Fig. 11b and Fig. 12b. However, when a signal passes through the channels, β is primarily influenced by the multi-path signals, which can be observed in Fig. 12b. The values of β tend to be stable because of the stable channel structures even though the amplitudes of multi-paths vary with time. With different inputs, the bounds
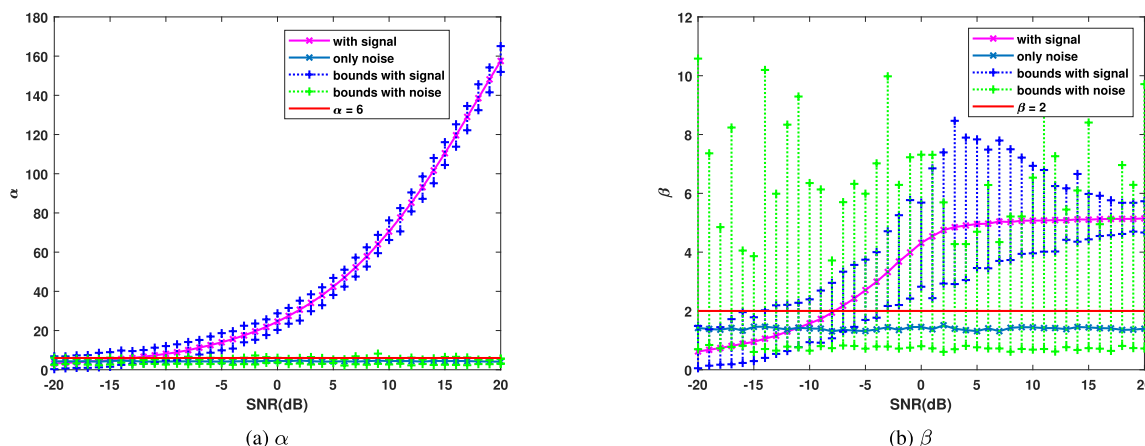

(a) α (b) β

FIGURE 11. The values of α and β with different inputs in AC Channel.

(a) α

(b) β
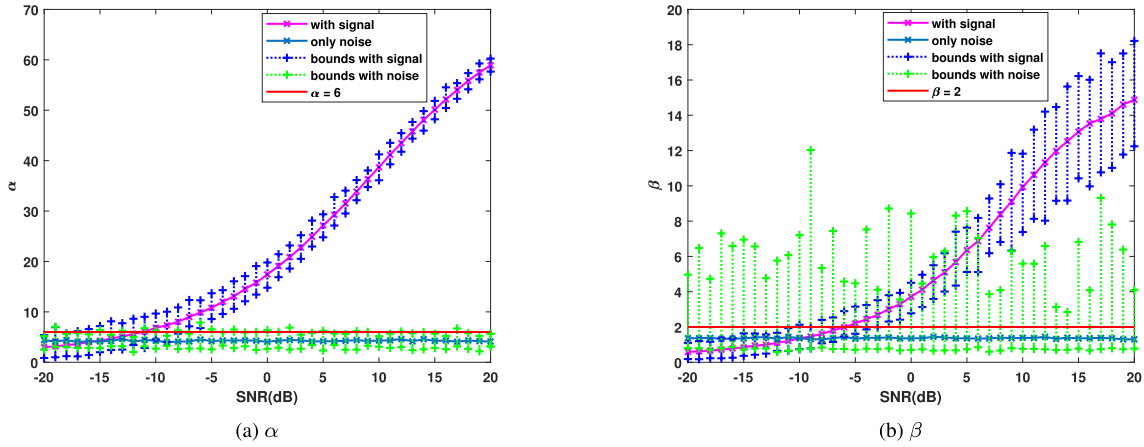
FIGURE 12. The values of α and β with different inputs in AS Channel.
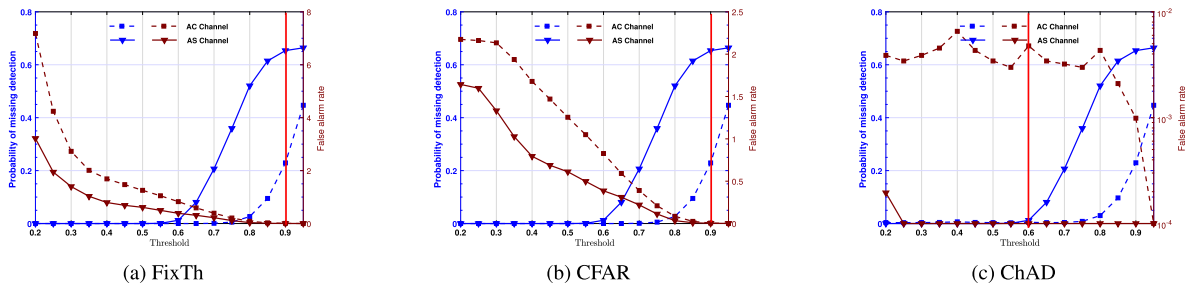

(a) FixTh

(b) CFAR

(c) ChAD

FIGURE 13. Performance with different thresholds at $0dB$.

of β are partly overlap, especially at low SNRs. It means that noise may be falsely detected as signal when a fixed β is used as a decision criterion, resulting in P_{FA} increasing. Therefore, a higher β is more appropriate to obtain a lower P_{FA}. Considering that a higher β will result in a lower P_D, we should get a high P_D and low P_{FA} at the same time. Since the LaJD procedure is used to further decrease P_{FA}, we set $\beta^* = 2$ so that the wake-up signal can be detected at a low SNR.

In order to get V_{th}^*, we consider two conventional methods as benchmarks for comparison. One is FixTh [7], which is RC-based method with fixed threshold; and the other is CFAR [15], which is with the mechanism for constant false alarm rate. Our approaches are termed as ChAD and ChAD-LaJD, respectively. ChAD and ChAD-LaJD are with the same LFM signal detection methods, so we only evaluate ChAD in this subsection. To illustrate more clearly, Fig. 13 shows the probability of missing detection $1 - P_D$ instead of P_D and false alarm rate P_{FA} with different thresholds V_{th} at $0dB$ given the optimal values $\alpha^* = 6$ and $\beta^* = 2$. For the convenience of expression, we denote $1 - P_D$ as P_{MD}. Compared with conventional performance criteria, P_{FA} defined in this paper may be more than 1 because that several peaks might satisfy the predefined detection conditions for each LFM signal. As shown in Fig. 13, at the same threshold V_{th}, P_{FA} in AC Channel is lower than the one in AS Channel. On the other hand, P_{MD} in AC Channel is higher than the one in AS Channel. However, we do not need to compare

the performances under the two channel models. What we consider is how to select an optimal value of V_{th}^* which guarantees both low P_{FA} and P_{MD} under the two channel models. As far as both are considered, P_{FA} should get more attention in detection procedure because that P_{MD} will be further considered in the joint decision procedure. As for FixTh method, P_{FA} decreases to less than 10^{-2} when V_{th} is more than 0.9 under the two channel models. The performance of CFAR is similar to the one of FixTh. So we choose 0.9 as V_{th}^* for FixTh and CFAR. Compared with two conventional methods, P_{FA} of ChAD is comparative lower and less than 10^{-2} in all thresholds. Jointly considering P_{FA} and P_{MD}, we choose 0.6 as V_{th}^* for ChAD and ChAD-LaJD. It is interesting that a lower value of V_{th} is feasible for our detection approach.

Now, we have obtained the optimal parameter set $\{V_{th}^*, \alpha^*, \beta^*\}$. As in the two conventional methods, the values are $\{0.9, 6, 2\}$. As in our proposed methods ChAD and ChAD-LaJD, the values are $\{0.6, 6, 2\}$. The performances will be evaluated in the sequent subsection based on the optimal parameter values.

C. DETECTION PROBABILITY AND FALSE ALARM RATE
We evaluate the performance of the wake-up system in AC Channel and AS Channel given the optimal parameter set $\{V_{th}^*, \alpha^*, \beta^*\}$. Fig. 14 and Fig. 15 show the performance v.s. SNR under the two channel models, respectively.
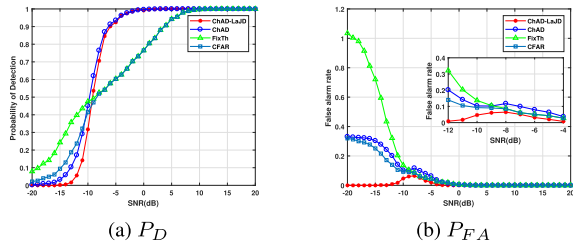
(a) P_D

(b) P_{FA}

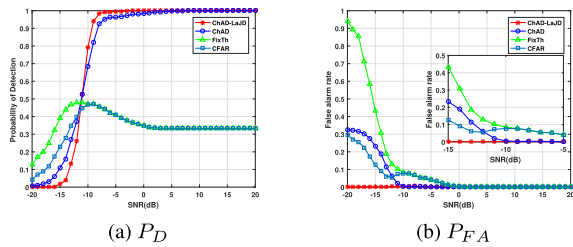**FIGURE 14.** The Performance in AC Channel.

(a) P_D

(b) P_{FA}

FIGURE 15. The performance in AS Channel.

As shown in Fig. 14a, when SNR is more than $-10dB$, ChAD and ChAD-LaJD are with higher P_D than two conventional methods in AC Channel. Moreover, more than 90% wake-up signals are detected when SNR is higher than $-5dB$.

Fig. 14b shows the performance of P_{FA} in AC Channel. ChAD-LaJD outperforms FixTH and CFAR at all SNRs. At most SNRs from $-20dB$ to $20dB$, P_{FA} of ChAD-LaJD has dropped to below 10^{-3}. However, a peak point exists at $-8dB$. This can be explained by the channel characteristics and the decision conditions defined in Equ. (10). AC Channel is featured with complex multi-path structure, in which there are many multi-paths whose power are not low. So the multi-paths are probably falsely detected. When SNR is lower than $-10dB$, the multi-paths are overwhelmed by the noise. Aided by the noise, the condition $V_{pp} > V_{th}^*$ is satisfied. However, the conditions $\hat{\alpha} > \alpha^*$ and $\hat{\beta} > \beta^*$ are both not satisfied. As a result, the multi-paths will not be falsely detected. As SNR increases, the power of noise decreases and the condition $\hat{\alpha} > \alpha^*$ becomes true prior to the condition $\hat{\beta} > \beta^*$, referring to Fig. 11b. In this situation, the conditions $\hat{\alpha} > \alpha^*$ and $\hat{\beta} > \beta^*$ are both satisfied. Thus, the multi-paths are probably falsely detected. When SNR further increases, V_{pp} is only decided by the power of the multi-path, and then the condition outputs of $V_{pp} > V_{th}^*$ are false. As a result, the multi-paths will not be falsely detected.

Fig. 15 shows the performance under AS Channel which has different multi-path structure compared with AC Channel. In AS Channel, the powers of multi-paths vary severely even in the duration of a wake-up signal. So three LFMs in a wake-up signal experience different attenuations. As for FixTh and CFAR, V_{th}^* is 0.9, which is a comparatively high value. Two LFMs cannot be detected because the receive signal power is lower than V_{th}^*. This conclusion can be verified by Fig. 15a. As SNR increases, P_D increases and arrives at a peak point aided by noise, and then drops to a fixed value of 0.33. The performances of ChAD and ChAD-LaJD are not

influenced by the signal attenuation because that V_{th}^* is low. Similarly to AC Channel, more than 90% wake-up signals are detected when SNR is higher than $-5dB$.

Compared with AC Channel, the powers of multi-paths are much lower than the main path in AS Chanel. The characteristic is embodied by the performance of P_{FA} shown in Fig. 15b. As SNR increases, P_{FA} of ChAD and ChAD-LaJD decreases. Specifically, P_{FA} of ChAD-LaJD is stable and lower than 10^{-3} at any SNR. These results can be explained by the parameter β which reflects the influence of multi-paths. Low power multi-paths cannot trigger the condition $\hat{\beta} > \beta^*$ in ChAD and ChAD-LaJD. Different from other methods, P_{FA} of CFAR experiences the procedure of first increasing and then decreasing. These results are similar to the ones of ChAD in AC Channel. Compared with ChAD, the detection results of CFAR are constrained by two conditions $V_{pp} > V_{th}^*$ and $\hat{\alpha} > \alpha^*$ except for the condition $\hat{\beta} > \beta^*$. Aided by the condition $\hat{\alpha} > \alpha^*$, P_{FA} of CFAR is lower than the one of FixTh at the same SNR. But with the increase of SNR, the effects of the condition decrease. So when SNR is more than $-10dB$, the performance is the same as the one of FixTh.
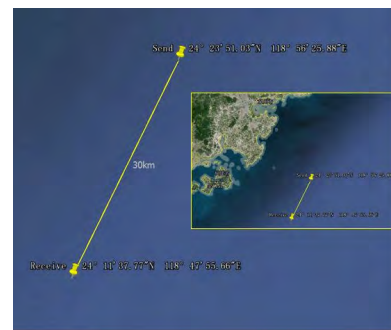

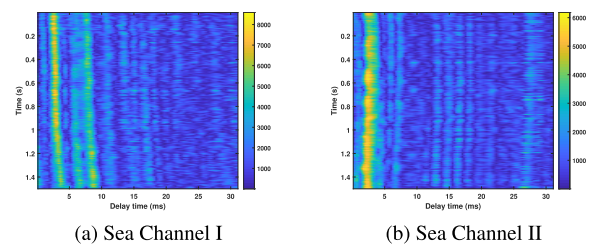**FIGURE 16.** The deployment of sea trial at Taiwan Strait.

(a) Sea Channel I

(b) Sea Channel II

FIGURE 17. The CIRs sounded from sea trials.

V. SEA AND LAKE TRIALS
A. SEA TRIALS
In this section, we evaluate our approaches applying sea channels sounded from sea trials at Taiwan strait on July, 2014. The deployment is depicted in Fig. 16. The transmission range is $30km$; and the water depth is $50m$. The CIRs, referred to as Sea Channel I and Sea Channel II, are illustrated in Fig. 17. We can find that the channels are featured with simple multi-path structure but influenced by Doppler effect.

The parameters of the wake-up signal are the same as the ones in the simulations. After a wake-up signal passes
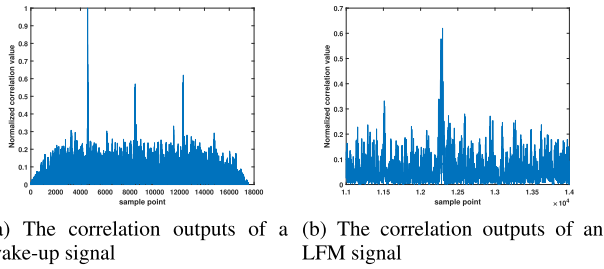
(a) The correlation outputs of a wake-up signal
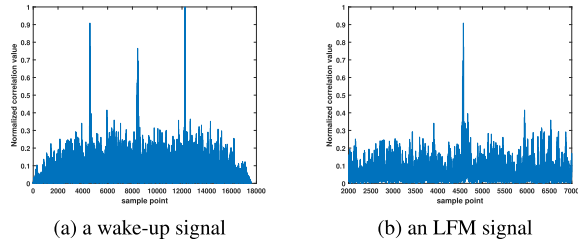
(b) The correlation outputs of an LFM signal

FIGURE 18. Correlation outputs in Sea Channel I.

(a) a wake-up signal

(b) an LFM signal

FIGURE 19. Correlation outputs in Sea Channel II.

(a) P_D

(b) P_{FA}
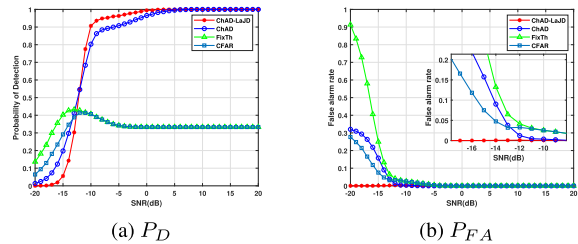
FIGURE 20. Detection performance in Sea channel I.
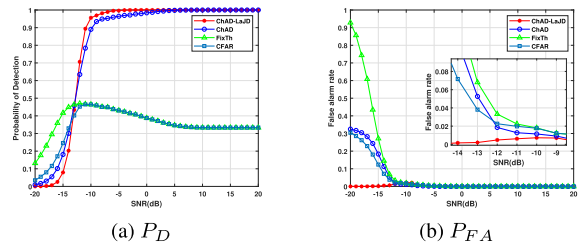

(a) P_D

(b) P_{FA}

FIGURE 21. Detection performance in Sea channel II.

through the sea channels, the received signals are added band-limited Gaussian noise with different SNRs. After correlated with the replica of the transmitted signals, the correlation outputs corresponding to Sea Channel I and II are shown in Fig. 18 and Fig. 19, respectively. We can find that different LFM signals in a wake-up signal experience different amplitude attenuations.

In Section IV, we have obtained the optimal parameter sets $\{V_{th}^*, \alpha^*, \beta^*\}$ for different methods. In this section, we use $\{0.6, 6, 2\}$ and $\{0.9, 6, 2\}$ as the parameter sets for our approaches and the conventional methods, respectively.

Fig. 20 and Fig. 21 show the detection performance in Sea Channel I and Sea Channel II, respectively. Compared with the conventional methods, P_D of our approaches is much higher when SNR is more than $-12dB$ and is close to

100% when SNR is over $0dB$. While P_D of the conventional methods reaches a performance floor at 0.33 when SNR is over $-5dB$. The results are similar to the ones in AS Channel of the simulations. As V_{th}^* is set as 0.9 in the simple decision criteria of the conventional methods, the correlation outputs of the latter two LFM signals are below the fixed threshold because of Doppler distortion when SNR is high. On the contrary, the correlation outputs of the fading LFM signals may be more than V_{th}^* aided by noises when SNR is low. The P_{FA} of ChAD-LaJD is better than other methods and reaches below 0.01 at all SNRs because of its joint decision mechanism, which is featured with diversity characteristic. What should be noticed is that P_{FA} of ChAD-LaJD at Sea channel II is not monotonous and reaches the highest value when SNR is $-9dB$. It means that more signals are falsely alarmed with the increase of SNR when SNR is less than $-9dB$. It can be explained through its joint decision mechanism. As SNR increases, some false peaks satisfy the location relationship, and then the corresponding signals are detected as a wake-up signal. When SNR increases to more than $-9dB$, the number of false peaks decreases and the location relationship cannot be satisfied. However, P_{FA} is still below 0.01 and smaller than other methods even the monotony exists.

FIGURE 22. The deployment of lake trials at Danjiang Lake.

B. LAKE TRIALS

The lake trials are conducted at Danjiang Lake in Henan province of China in September, 2018. Fig. 22 shows the deployment of the lake trials. The transmission range is $2.72km$ and the water depth is $40m$. The transmitter is deployed at the depth of $20m$. Multiple hydrophones are used to receive the signals. The signals are transmitted packet by packet. There are 10 wake-up signals in each packet, and the first wake-up signal in each packet is used as synchronization. In total, 10 packets are transmitted, and 81 wake-up signals and 243 LFMs are received. The system parameter sets are briefly shown in TABLE 2.

A wake-up signal for transmitting and its corresponding received signal in time domain are shown in Fig. 23a and Fig. 23b. We can find that the SNR of the received signal is not high. It is difficult to distinguish signals and noises. But we can obtain the bandwidth of signals plotted by two red lines from the power spectral density shown in Fig. 23c and Fig. 23d.

Fig. 24 shows two typical CIRs of the lake trials referred to as Lake Channel I and II, respectively. Compared with sea trials, the CIRs of lake trials are featured with more complicated

TABLE 2. The system parameters of lake trials.

Parameters	Values
Number of packets	10
Number of wake-up signals of a packet	10
Number of LFMs of a wake-up signal	3
Length of each LFM T_S (ms)	85.33
Guard interval T_G (ms)	42.67
Center frequency f_c (kHz)	6
Bandwidth B (kHz)	3
Sample rate f_s (kHz)	48

(a) Transmitted in time-domain   (b) Received in time-domain

(c) Transmitted in frequency-domain   (d) Received in frequency-domain
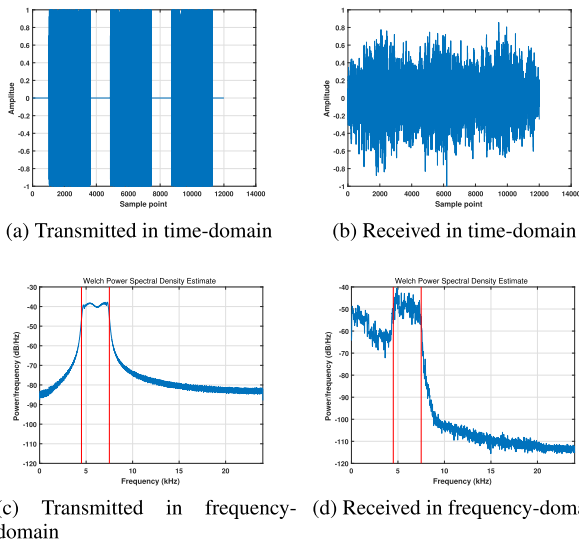
FIGURE 23. A transmitted and received wake-up signal.

(a) Lake Channel I   (b) Lake Channel II
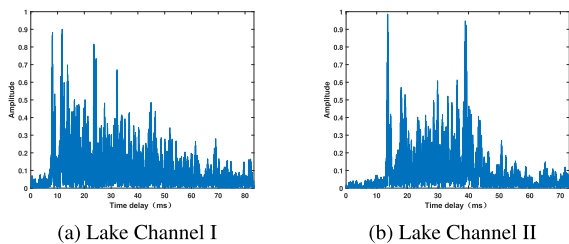
FIGURE 24. Two typical channel impulse responses at lake trials.

FIGURE 25. A wake-up signal in lake Channel I.

FIGURE 26. A wake-up signal in lake Channel II.

TABLE 3. The number of detected signals in lake trail.

Channel No.	ChAD-LaJD	ChAD	CFAR	FixTh
1	81	243	170	170
2	81	241	242	242
3	76	237	221	221
4	66	209	203	203
5	81	241	162	162
6	76	409	208	208

multi-path structure. As shown in Fig. 24a, the multi-path spread of Lake Channel I is long up to 70*ms*, and its amplitudes are with exponential distribution, which is prone to resulting in false alarm in conventional methods. Moreover, some multi-paths with comparative high amplitudes arrive before the strongest path (referred to as the main path), which will do harm to the detection of the main path. Lake Channel II is another type of CIR different from Lake Channel I. As shown in Fig. 24b, there are two strong multi-paths within a non-short interval. The second multi-path will also wake up the receiver as same as the first multi-path, resulting in false alarm in FixTh, CFAR and ChAD methods.

Influenced by the CIRs mentioned above, Fig. 25 and Fig. 26 show the detection results of a wake-up signal in Lake Channel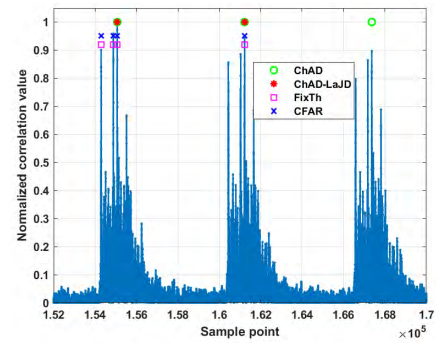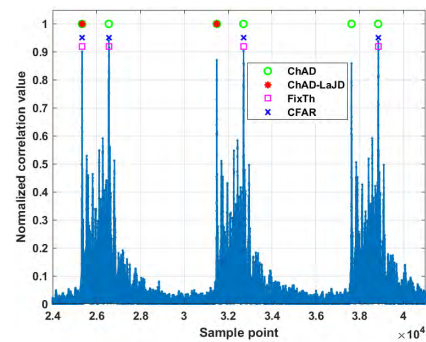 I and II, respectively. We can find that the wake-up signal detection is mainly affected by the multi-path structure. In Fig. 25, several peaks are detected when an LFM signal is obtained in FixTh and CFAR methods because of strong multi-paths. Sometimes none are detected. While in ChAD and ChAD-LaJD approaches, one and only one peak is detected. It means that our approaches are effective as long as the highest amplitude of the main path is β^* times the one of the multi-paths. For ChAD-LaJD, only the first two peaks are marked because that the two peaks are enough to detect a wake-up signal successfully.

In Fig. 26, as discussed for CIRs of Lake Channel II, two strong multi-paths both arrive in an LFM signal. Thus, two peaks are detected in ChAD approach. In this case, ChAD-LaJD characterized with joint decision still can deal with it because the false alarm will be ignored due to its false location relationship.

TABLE 3 shows the detected number of signals at each channel. A channel in this paper is corresponding to a hydrophone. Ideally, 81 wake-up signals should be detected in ChAD-LaJD approach and 243 LFM signals should be

detected in other approaches. As shown in TABLE 3, CFAR and FixTh are with similar performance because that the multi-path structure is the main factor compared with the noise. It is corresponding with the channel states discussed above. Considering the six channels, the detected numbers vary differently. Among these methods, ChAD and ChAD-LaJD are more robust. In particular, the detected number of ChAD in the sixth channel is 409, which is much greater than other channels. But the detected number of ChAD-LaJD is not affected and keeps a normal level of 76. It means that ChAD-LaJD is effective in the channels with complicated multi-path structure.

VI. CONCLUSIONS

In this paper, we propose a wake-up signal detection approach called ChAD-LaJD for UAC terminals. ChAD-LaJD applies a group of LFMs as a wake-up signal and consists of two parts: ChAD and LaJD. In ChAD, two special parameters besides a fixed threshold are defined to improve the adaptability to channels. In LaJD, location relationship of LFM signals is utilized to form diversity characteristics. The simulations under two different channel models show that a comparative low fixed threshold is reliable to get a lower P_{FA} compared with the conventional detection methods. The sea and lake trials are also conducted to evaluate the performance of ChAD-LaJD. In sea trials with transmission range $30km$, the channels are with simple multi-path structure but with Doppler effect. The value of P_D of ChAD-LaJD reaches close to 100% when SNR is more than $0dB$; while the conventional methods reach a performance floor of 0.33. Furthermore, P_{FA} of ChAD-LaJD is better than other methods and reaches below 10^{-2} even when SNR is $-20dB$. In lake trials with transmission range $2.72km$, the channels are with complicated multi-path structure but without Doppler effect. The detected peaks of one wake-up signal and the number of detected wake-up signals show that ChAD-LaJD works quite well under the complicated multi-path channels.

ACKNOWLEDGMENT

REFERENCES

[1] H. Jindal, S. Saxena, and S. Singh, "Challenges and issues in underwater acoustics sensor networks: A review," in *Proc. Int. Conf. Parallel, Distrib. Grid Comput.*, Solan, India, Dec. 2015, pp. 251–255.

[2] M. Chitre, S. Shahabudeen, L. Freitag, and M. Stojanovic, "Recent advances in underwater acoustic communications & networking," in *Proc. OCEANS*, Quebec City, QC, Canada, Sep. 2008, pp. 1–10.

[3] R. Su, R. Venkatesan, and C. Li, "An energy-efficient asynchronous wake-up scheme for underwater acoustic sensor networks," *Wireless Commun. Mobile Comput.*, vol. 16, no. 9, pp. 1158–1172, Jun. 2016.

[4] P. Qarabaqi and M. Stojanovic, "Statistical characterization and computationally efficient modeling of a class of underwater acoustic communication channels," *IEEE J. Ocean. Eng.*, vol. 38, no. 4, pp. 701–717, Oct. 2013.

[5] A. Sánchez, S. Blanc, P. Yuste, and J. J. Serrano, "RFID based acoustic wake-up system for underwater sensor networks," in *Proc. IEEE 8th Int. Conf. Mobile Ad-Hoc Sensor Syst.*, Valencia, Spain, Oct. 2011, pp. 873–878.

[6] Z. Cuixia, W. Jiaxin, and L. Yuanxuan, "Design of low-power wake-up circuits in underwater acoustic communication," *Phys. Procedia*, vol. 33, pp. 884–891, Jan. 2012.

[7] M. Yue, Y. R. Zheng, Z. Chen, and Y. Han, "Microcontroller implementation of low-complexity wake-up receiver for wireless sensor nodes in severe multipath fading channels," in *Proc. IEEE/OES China Ocean Acoust. (COA)*, Harbin, China, Jan. 2016, pp. 1–6.

[8] Z. Guo, S. Yan, and L. Xu, "A new method for frame synchronization in acoustic communication," in *Proc. OCEANS*, Shanghai, China, Apr. 2016, pp. 1–6.

[9] R. Pec, M. S. Khan, and Y. S. Cho, "An LFM-based preamble for underwater communication," in *Proc. Int. Conf. Inf. Commun. Technol. Converg. (ICTC)*, Jeju, South Korea, Oct. 2017, pp. 1181–1183.

[10] W. Lei, D. Wang, Y. Xie, B. Chen, X. Hu, and H. Chen, "Implementation of a high reliable chirp underwater acoustic modem," in *Proc. OCEANS*, Yeosu, South Korea, May 2012, pp. 1–5.

[11] Y. Zhao, H. Yu, G. Wei, F. Ji, and F. Chen, "Parameter estimation of wideband underwater acoustic multipath channels based on fractional Fourier transform," *IEEE Trans. Signal Process.*, vol. 64, no. 20, pp. 5396–5408, Oct. 2016.

[12] P. M. Baggenstoss, "On detecting linear frequency modulated waveforms in dispersive channels: Alternatives to segmented replica correlation," *IEEE J. Ocean. Eng.*, vol. 19, no. 4, pp. 591–598, Oct. 1994.

[13] B. Friedlander and A. Zeira, "Detection of broadband signals in frequency and time dispersive channels," *IEEE Trans. Signal Process.*, vol. 44, no. 7, pp. 1613–1622, Jul. 1996.

[14] L. B. Almeida, "The fractional Fourier transform and time-frequency representations," *IEEE Trans. Signal Process.*, vol. 42, no. 11, pp. 3084–3091, Nov. 1994.

[15] M. A. Khalighi and M. H. Bastani, "Adaptive CFAR processor for nonhomogeneous environments," *IEEE Trans. Aerosp. Electron. Syst.*, vol. 36, no. 3, pp. 889–897, Jul. 2000.

[16] T. B. Santoso, M. Huda, and H. Mahmudah, "Performance evaluation of CFAR detector for delay spread analysis of underwater acoustic channel," in *Proc. Int. Electron. Symp. (IES)*, Surabaya, Indonesia, Sep. 2015, pp. 173–177.

[17] H. Kim, J. Seo, J. Ahn, and J. Chung, "Snapping shrimp noise mitigation based on statistical detection in underwater acoustic orthogonal frequency division multiplexing systems," *Jpn. J. Appl. Phys.*, vol. 56, no. 7, Jun. 2017, Art. no. 07JG02.

[18] T. I. Incorporated. (2017). *Tms320c6748 Fixed- and Floating-Point DSP*. [Online]. Available: http://www.ti.com/lit/ds/symlink/tms320c6748.pdf

[19] T. I. Incorporated. (2019). *C6748/46/42 Power Consumption Summary*. [Online]. Available: http://www.ti.com/lit/an/sprabf9/sprabf9.pdf

[20] D. Zeng, S. Yan, L. Xu, and Z. Zhang, "The low power DSP platform design of underwater acoustic communication system," in *Proc. IEEE Int. Conf. Signal Process., Commun. Comput. (ICSPCC)*, Hong Kong, Aug. 2016, pp. 1–4.

[21] C. R. Berger, S. Zhou, J. C. Preisig, and P. Willett, "Sparse channel estimation for multicarrier underwater acoustic communication: From subspace methods to compressed sensing," *IEEE Trans. Signal Process.*, vol. 58, no. 3, pp. 1708–1721, Mar. 2010.

[22] T. I. Incorporated. (2019). *Msp430fr267x Capacitive Touch Sensing Mixed-Signal Microcontrollers*. [Online]. Available: http://www.ti.com/lit/ds/symlink/msp430fr2676.pdf
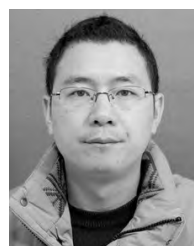
DEQING WANG received the Ph.D. degree in communication engineering from Xiamen University, China, in 2013. He was a Visiting Scholar with the Georgia Institute of Technology, from 2016 to 2017. He is currently an Assistant Professor with the Key Laboratory of Underwater Acoustic Communication and Marine Information Technology, Xiamen University, Ministry of Education, Xiamen, China. His research interests include underwater acoustic communication and networking, underwater acoustic signal processing, and underwater acoustic physical-layer network coding.

HAIYU LI received the B.S. degree in communication engineering from Xiamen University, China, in 2017, where he is currently pursuing the M.S. degree in communication engineering. His current research interest includes underwater acoustic physical-layer network coding.

XIAOYI HU received the M.S. degree in communication and information system from the Beijing Institute of Technology, China, in 1995. She was a Visiting Scholar with Connecticut State University, from 2013 to 2014. She is currently a Professorate Senior Engineer with the Key Laboratory of Underwater Acoustic Communication and Marine Information Technology, Xiamen University, Ministry of Education, Xiamen, China. Her research interests mainly include underwater acoustic communication, underwater acoustic signal processing, and embedded circuit system design.

LIQUN FU (S'08–M'11–SM'17) received the Ph.D. degree in information engineering from The Chinese University of Hong Kong, in 2010. She was a Postdoctoral Research Fellow with the Institute of Network Coding, The Chinese University of Hong Kong, and the ACCESS Linnaeus Centre, KTH Royal Institute of Technology, from 2011 to 2013 and from 2013 to 2015, respectively. She was an Assistant Professor with ShanghaiTech University, from 2015 to 2016. She is currently a Full Professor with the School of Informatics, Xiamen University, China. Her research interests mainly include communication theory, optimization theory, game theory, and learning theory, with applications in wireless networks. She serves as a TPC Member for many leading conferences in communications and networking, such as the IEEE INFOCOM, ICC, and GLOBECOM. She served as the Technical Program Co-Chair of the GCCCN Workshop of the IEEE INFOCOM 2014, the Publicity Co-Chair of the GSNC Workshop of the IEEE INFOCOM 2016, and the Web Chair of the IEEEWiOpt 2018. She is on the editorial board of IEEE Access and the JOURNAL OF COMMUNICATIONS AND INFORMATION NETWORKS (JCIN).

YONGJUN XIE received the M.S. degree in communication engineering from Xiamen University, China, in 2009, where he is currently a Senior Engineer with the Key Laboratory of Underwater Acoustic Communication and Marine Information Technology, Ministry of Education, Xiamen, China. His research interests mainly include underwater acoustic communication and embedded circuit system design.

• • •